A comparative study of Minimum Variance Distortionless Response beamforming, Linearly Constrained Minimum Variance beamforming and metaheuristic solved null-steering beamforming

Mr. Robert Macharia Maina and Dr. Kibet Lang'at and Dr. P. K. Kihato

Abstract—Digital beamforming is of paramount significance in addressing wireless communication systems' capacity enhancement. Among well established digital beamforming mechanisms are Minimum Variance Distortionless Response (MVDR) and Linearly Constrained Minimum Variance (LCMV) techniques. It would be worthwhile to establish the relative performance of the afore-mentioned techniques in beamforming in various situations. In this paper, MVDR and LCMV techniques performance comparison is addressed from the perspective of narrowband beamforming (in reception mode), with the variation parameter being signal/ interferer spatial separation. The LCMV beamformer has been constrained to yield nulls in interferer Direction of Arrivals (DoAs). Also studied is a Particle Swarm Optimization (PSO) solved null-steering beamformer. It is established that the PSO solved null-steering beamformer outperforms the LCMV and MVDR techniques. MATLAB software has been used as the simulation tool.

Keywords—Digital beamforming, Linearly Constrained Minimum Variance, Minimum Variance Distortionless Response, Null steering

I. INTRODUCTION

Beamforming in wireless communication systems is of paramount significance towards achieving capacity enhancement. Beamforming is essentially a spatial filtering action [1]. Among techniques utilized in digital beamforming are Minimum Variance Distortionless Response (MVDR) and Linearly Constrained Minimum Variance (LCMV) methods. Use of metaheuristics in beamforming procedures such as beam steering, null steering, reference signal aided beamforming among others is an active research area. Beamforming on the basis of MVDR, LCMV and null steering techniques is a focus of the work presented in this paper.

Essentially, a reception digital beamformer operates on the basis of weighting signals received at elements of a suitably designed array. Taking into consideration an M element antenna array, a digital reception beamformer output can be framed as per (1). Reference can be made to [1].

$$y = \bar{w}^H \bar{x} \tag{1}$$

In (1):

- y is the beamformer output.
- $\bar{w}$ is the beamformer weights vector (of size M).
- $\bar{x}$ is an M sized vector containing signals observed at the array elements.

Mr. Robert Macharia Maina, Department of Telecommunication and Information Engineering, JKUAT (e-mail: robertisaacm@gmail.com).

Dr. Kibet Lang'at, Department of Telecommunication and Information Engineering, JKUAT.

Dr. P. K. Kihato, Department of Electrical and Electronic Engineering, JKUAT.

II. MINIMUM VARIANCE DISTORTIONLESS RESPONSE BEAMFORMER

The MVDR beamformer is designed with an aim of minimizing undesired signal power (interference and noise) whilst simultaneously maintaining maximal response in the Direction of Arrival (DoA) of the desired signal. This can be expressed mathematically as per (2).

$$\text{Minimize} \qquad \bar{w}^H \bar{R}_{uu} \bar{w} \tag{2a}$$

$$\text{Subject to} \qquad \bar{w}^H \cdot \bar{a}_s = 1 \tag{2b}$$

In (2), R_{uu} is the undesired signal correlation matrix and $\bar{a}_s$ is the array response vector corresponding to the desired signal DoA.

Studies involving the MVDR beamforming technique can be found in [2]–[5].

III. LINEARLY CONSTRAINED MINIMUM VARIANCE BEAMFORMER

The LCMV beamformer is designed with an aim of minimizing the total output power of an array subject to some constraints: generate maximal gain in the desired signal DoA and generate minimal gain in the undesired signals DoAs.

Studies involving the LCMV beamforming technique can be found in [6]–[9].

IV. NULL STEERING BEAMFORMER

The null steering beamformer is designed with an aim of generating an array response with maximum gain the desired signal DoA and nulls in the undesired (interferer) signal DoAs.

(3a) gives the array response magnitude (AF_s) corresponding to the desired signal DoA. (3b) gives the array response magnitude (AF_n) corresponding to an interfering signal DoA. The null steering condition to be optimized can be expressed as per (4).

$$AF_s = \bar{w}^H \cdot \bar{a}(\theta_s) \tag{3a}$$

$$AF_n = \bar{w}^H \cdot \bar{a}(\theta_n) \tag{3b}$$

$$J(\bar{w}) = AF_s - AF_n = \bar{w}^H \cdot \bar{a}(\theta_s) - \bar{w}^H \cdot \bar{a}(\theta_n) \quad (4)$$

$J(\bar{w})$ in (4) can be optimized using a metaheuristic algorithm, an action carried out in this paper.

Studies involving the null steering beamforming technique can be found in [10], [11].

V. METHODOLOGY

The problem at hand is essentially a reception beamforming problem. A receive linear antenna array with 10 isotropic elements is utilized. The desired signal is framed as having a DoA of 0 degrees azimuth, 0 degrees elevation. Two interferers are implemented, whose DoAs are framed as per Table I.

TABLE I
INTERFERER DOAS.

	Interferer 1 DoA		Interferer 2 DoA	
	Azimuth	Elevation	Azimuth	Elevation
Trial 1	-30	0	30	0
Trial 2	-20	0	20	0
Trial 3	-10	0	10	0
Trial 4	-5	0	5	0

The desired signal is framed as a sinusoid as per Fig. 1.

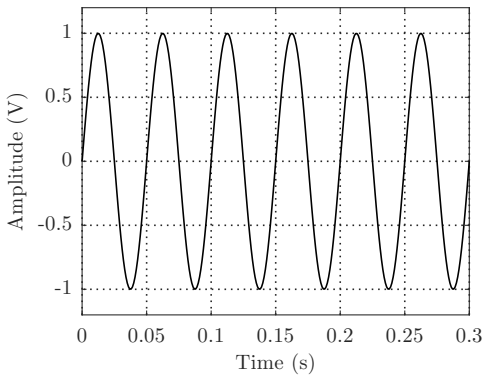

Fig. 1. Desired signal.

The interferes are framed as random signals as per Figs. 2 and 3.

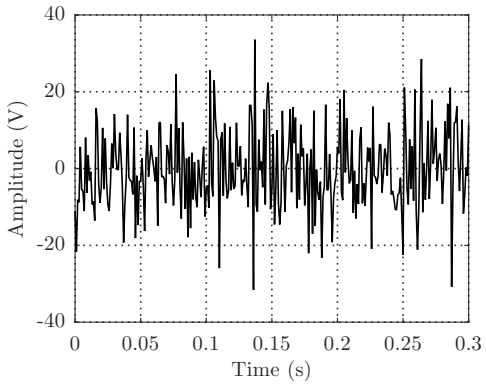

Fig. 2. Interferer 1.

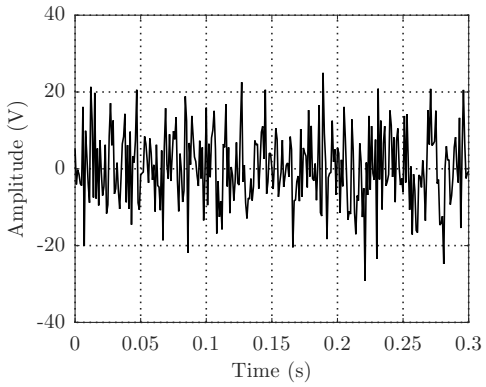

Fig. 3. Interferer 2.

A noisy channel resulting in a Signal to Noise Ratio (SNR) figure of 50dB is implemented. MVDR, LCMV, and Particle Swarm Optimization (PSO) solved null-steering beamforming schemes are utilized in solving the beamforming problem at hand. The LCMV beamformer has been constrained to yield nulls in interferer DoAs. A comparative study among the beamforming schemes is carried out with angular interferer separation as the study variable.

VI. RESULTS

The comparative study results are herein presented. The first trial results are comprehensively presented (including graphical presentations of signals received at each array element). For reasons of brevity, the other trial results are concisely presented.

A. Trial 1: 60 degrees interferer separation

The signals observed at the array elements are as per Fig. 4 to Fig. 13.

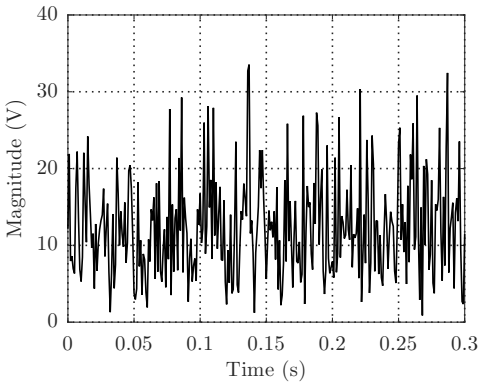

Fig. 4. Signal observed at array element 1.

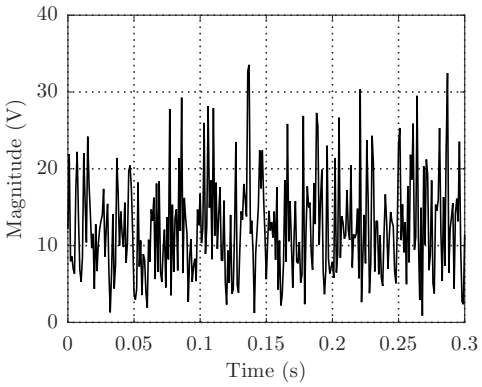

Fig. 5. Signal observed at array element 2.

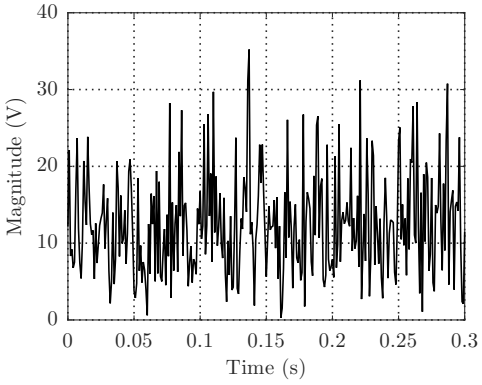

Fig. 6. Signal observed at array element 3.

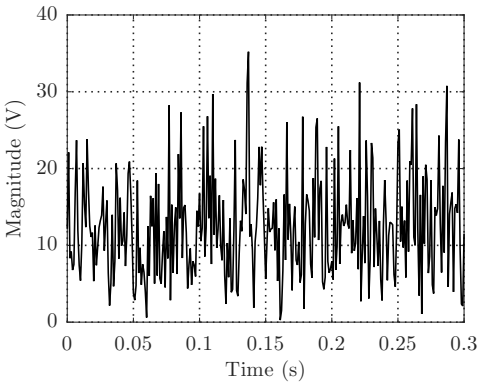

Fig. 7. Signal observed at array element 4.

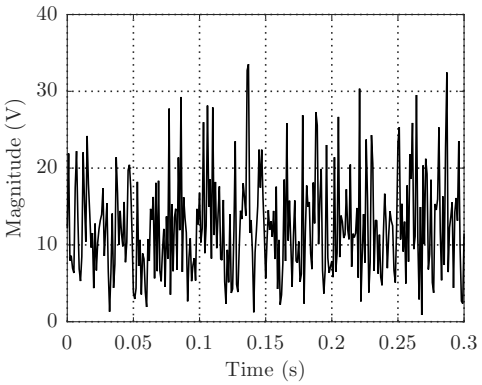

Fig. 8. Signal observed at array element 5.

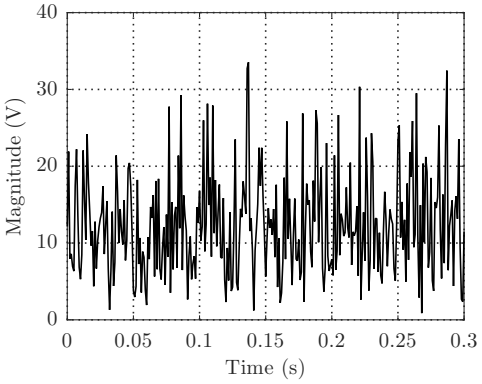

Fig. 9. Signal observed at array element 6.

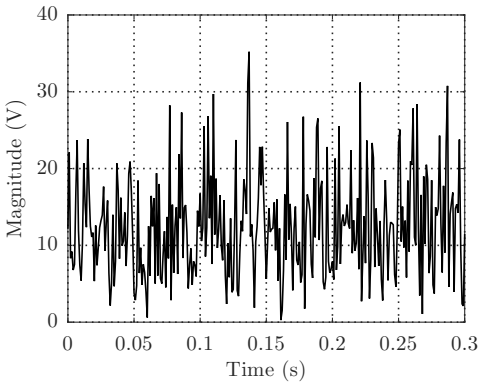

Fig. 10. Signal observed at array element 7.

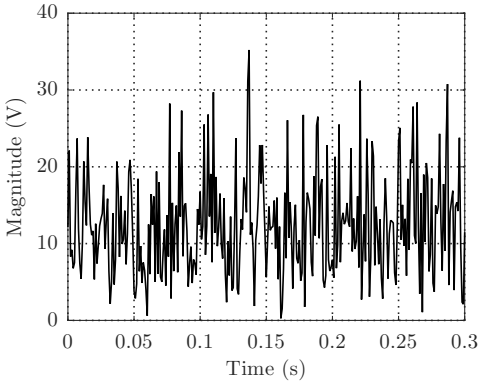

Fig. 11. Signal observed at array element 8.

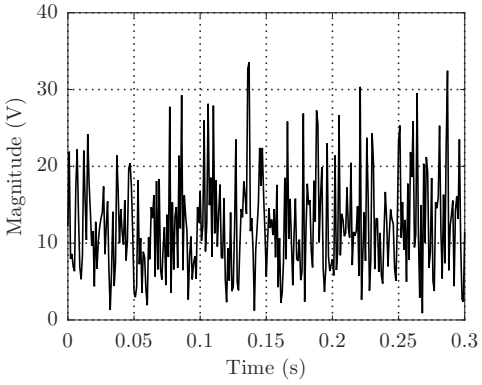

Fig. 12. Signal observed at array element 9.

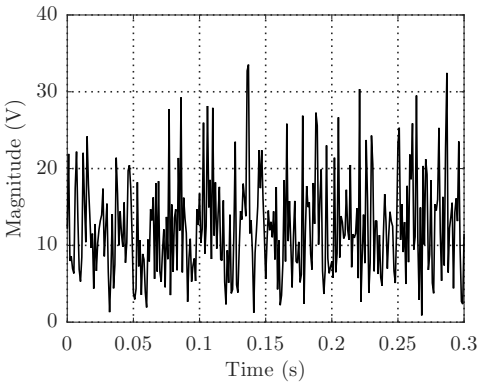

Fig. 13. Signal observed at array element 10.

Upon beamforming using the MVDR beamformer, the signal observed at the beamformer output is as per Fig. 14.

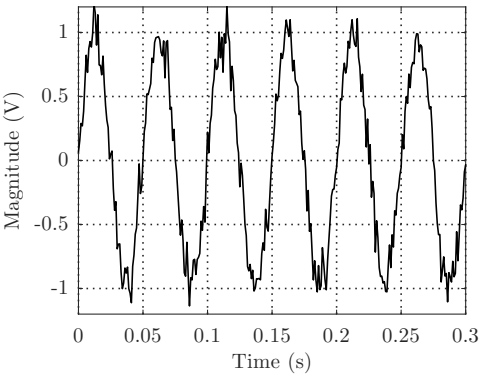

Fig. 14. Signal observed at beamformer output upon using the MVDR beamformer.

The MVDR beamformer resultant array response pattern is as per Fig. 15.

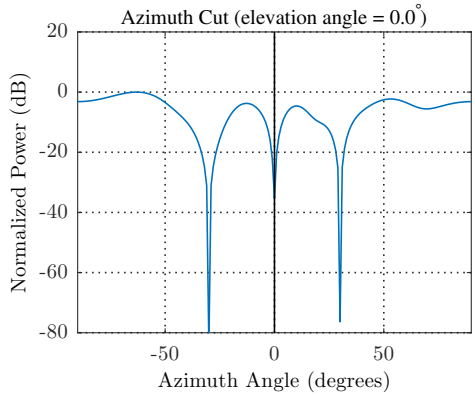

Fig. 15. Beamformer array response upon using the MVDR beamformer.

Upon beamforming using the LCMV beamformer, the signal observed at the beamformer output is as per Fig. 16.

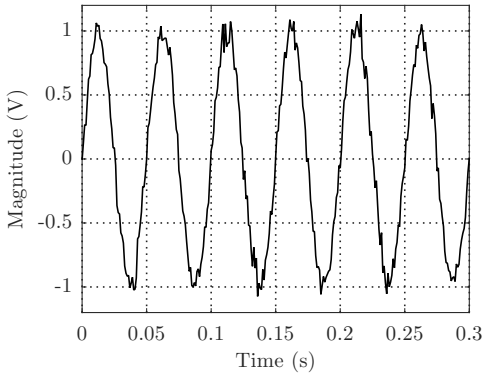

Fig. 16. Signal observed at beamformer output upon using the LCMV beamformer.

The LCMV beamformer resultant array response pattern is as per Fig. 17.

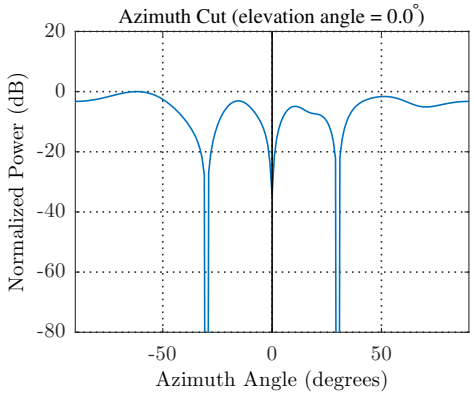

Fig. 17. Beamformer array response upon using the LCMV beamformer.

Upon beamforming using the PSO beamformer, the signal observed at the beamformer output is as per Fig. 18.

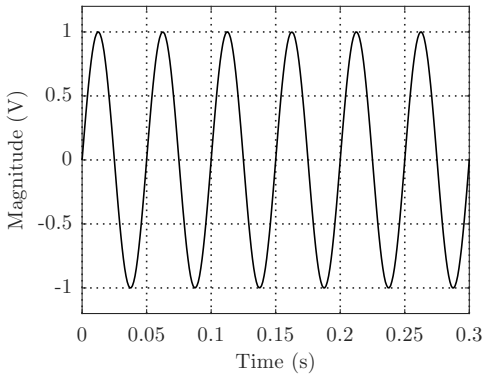

Fig. 18. Signal observed at beamformer output upon using the PSO beamformer.

The PSO beamformer resultant array response pattern is as per Fig. 19.

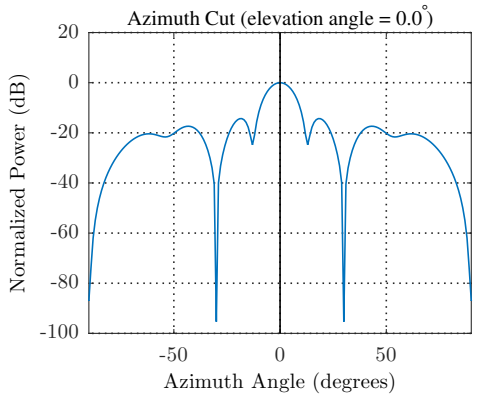

Fig. 19. Beamformer array response upon using the PSO beamformer.

Fig. 20 presents a comparative array response plot.

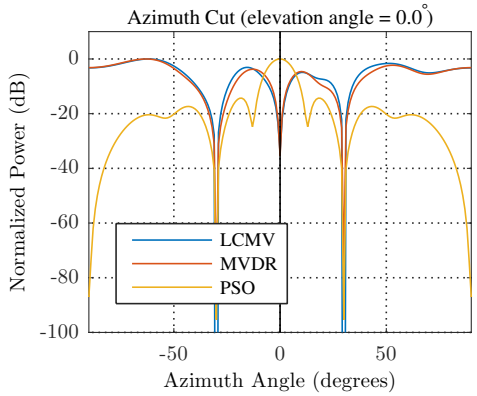

Fig. 20. Comparative array response plot.

From Fig. 20, it is easy to note the superior performance of the PSO solved null-steering beamformer over the MVDR and LCMV beamformers.

B. Trial 2: 40 degrees interferer separation

Upon beamforming using the MVDR beamformer, the signal observed at the beamformer output is as per Fig. 21.

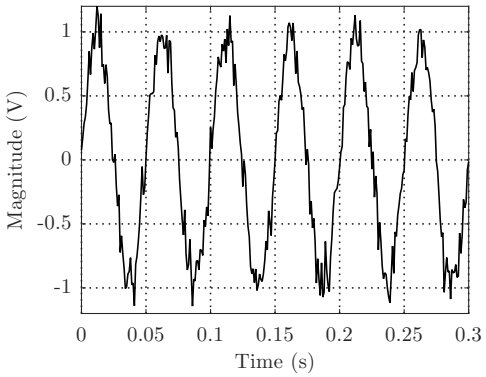

Fig. 21. Signal observed at beamformer output upon using the MVDR beamformer.

The MVDR beamformer resultant array response pattern is as per Fig. 22.

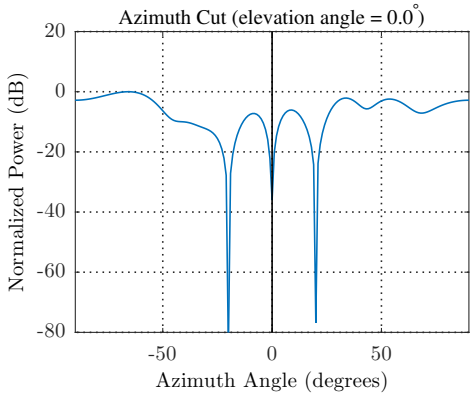

Fig. 22. Beamformer array response upon using the MVDR beamformer.

Upon beamforming using the LCMV beamformer, the signal observed at the beamformer output is as per Fig. 23.

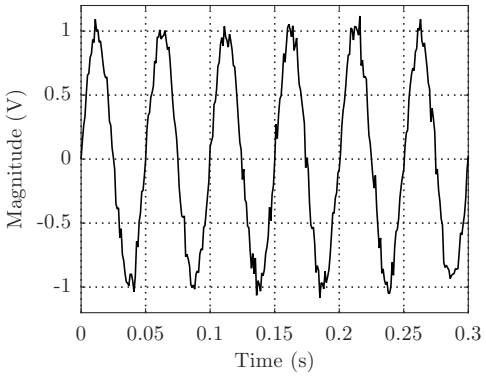

Fig. 23. Signal observed at beamformer output upon using the LCMV beamformer.

The LCMV beamformer resultant array response pattern is as per Fig. 24.

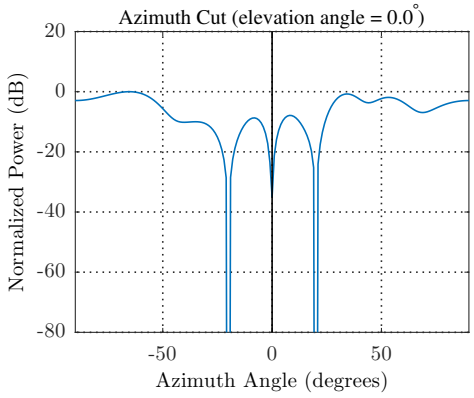

Fig. 24. Beamformer array response upon using the LCMV beamformer.

Upon beamforming using the PSO beamformer, the signal observed at the beamformer output is as per Fig. 25.

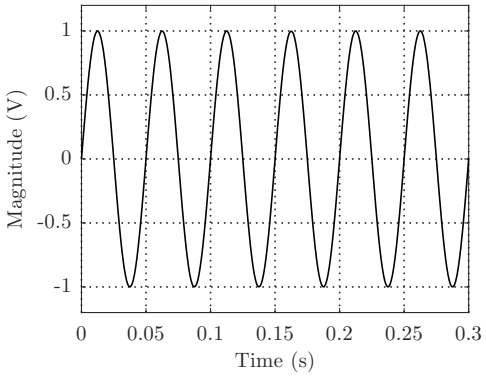

Fig. 25. Signal observed at beamformer output upon using the PSO beamformer.

The PSO beamformer resultant array response pattern is as per Fig. 26.

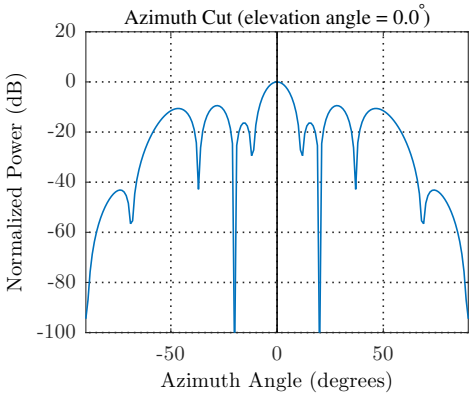

Fig. 26. Beamformer array response upon using the PSO beamformer.

Fig. 27 presents a comparative array response plot.

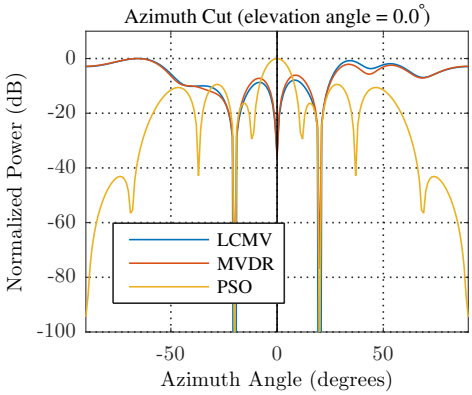

Fig. 27. Comparative array response plot.

From Fig. 27, it is easy to note the superior performance of the PSO solved null-steering beamformer over the MVDR and LCMV beamformers.

C. Trial 3: 20 degrees interferer separation

Upon beamforming using the MVDR beamformer, the signal observed at the beamformer output is as per Fig. 28.

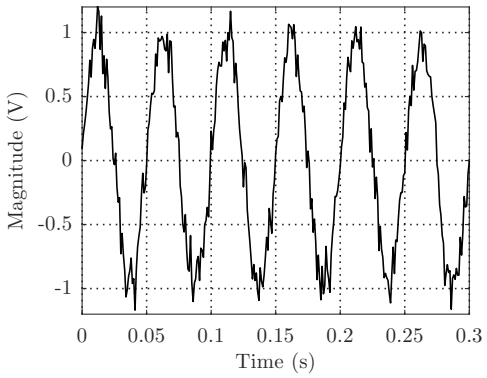

Fig. 28. Signal observed at beamformer output upon using the MVDR beamformer.

The MVDR beamformer resultant array response pattern is as per Fig. 29.

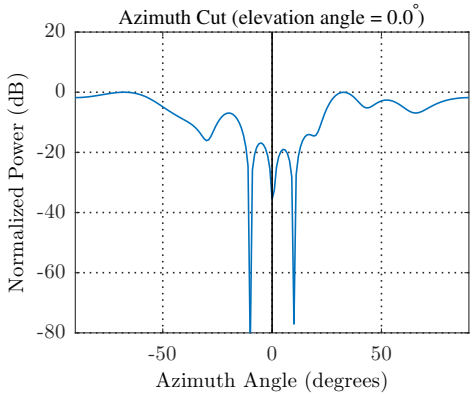

Fig. 29. Beamformer array response upon using the MVDR beamformer.

Upon beamforming using the LCMV beamformer, the signal observed at the beamformer output is as per Fig. 30.

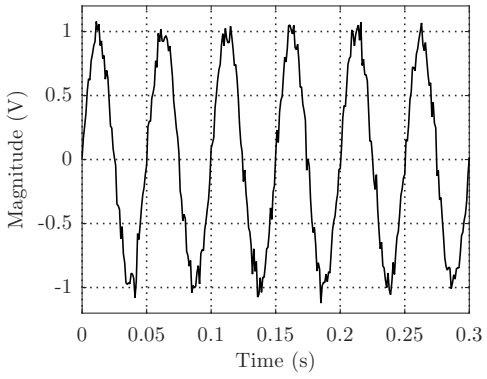

Fig. 30. Signal observed at beamformer output upon using the LCMV beamformer.

The LCMV beamformer resultant array response pattern is as per Fig. 31.

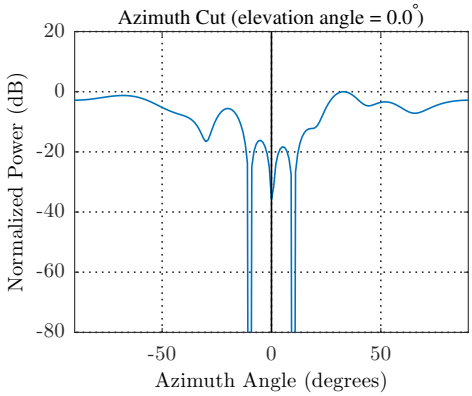

Fig. 31. Beamformer array response upon using the LCMV beamformer.

Upon beamforming using the PSO beamformer, the signal observed at the beamformer output is as per Fig. 32.

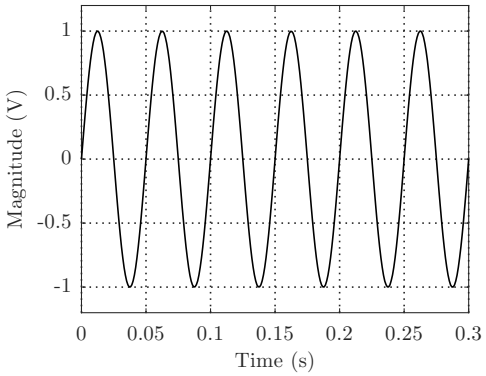

Fig. 32. Signal observed at beamformer output upon using the PSO beamformer.

The PSO beamformer resultant array response pattern is as per Fig. 33.

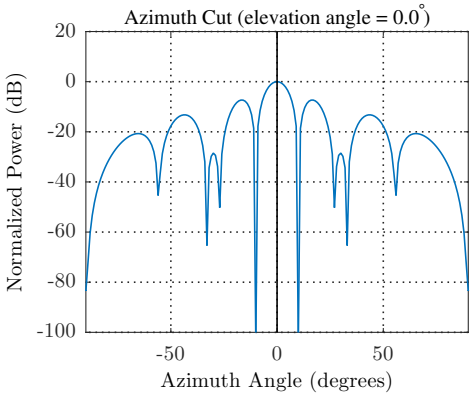

Fig. 33. Beamformer array response upon using the PSO beamformer.

Fig. 34 presents a comparative array response plot.

From Fig. 34, it is easy to note the superior performance of the PSO solved null-steering beamformer over the MVDR and LCMV beamformers.

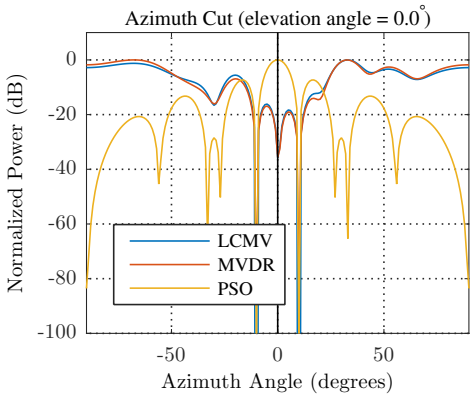

Fig. 34. Comparative array response plot.

D. Trial 4: 10 degrees interferer separation

Upon beamforming using the MVDR beamformer, the signal observed at the beamformer output is as per Fig. 35.

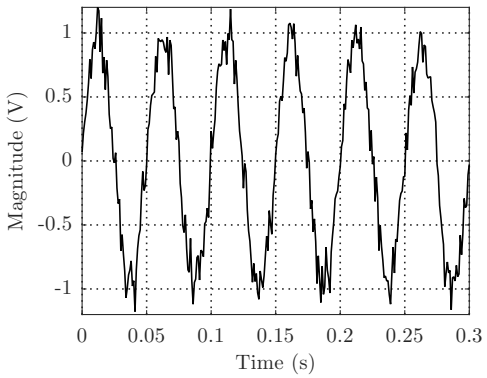

Fig. 35. Signal observed at beamformer output upon using the MVDR beamformer.

The MVDR beamformer resultant array response pattern is as per Fig. 36.

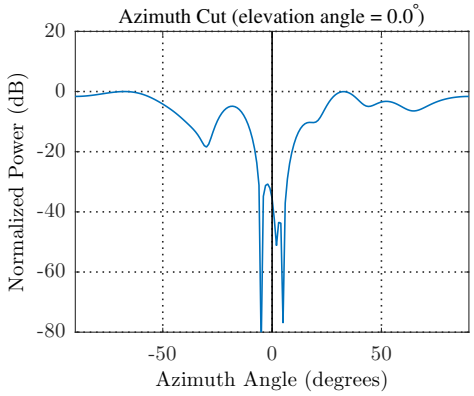

Fig. 36. Beamformer array response upon using the MVDR beamformer.

Upon beamforming using the LCMV beamformer, the signal observed at the beamformer output is as per Fig. 37.

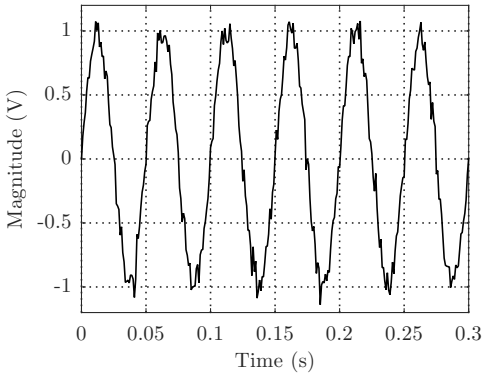

Fig. 37. Signal observed at beamformer output upon using the LCMV beamformer.

The LCMV beamformer resultant array response pattern is as per Fig. 38.

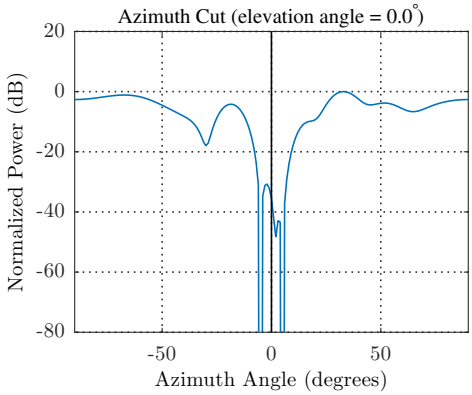

Fig. 38. Beamformer array response upon using the LCMV beamformer.

Upon beamforming using the PSO beamformer, the signal observed at the beamformer output is as per Fig. 39.

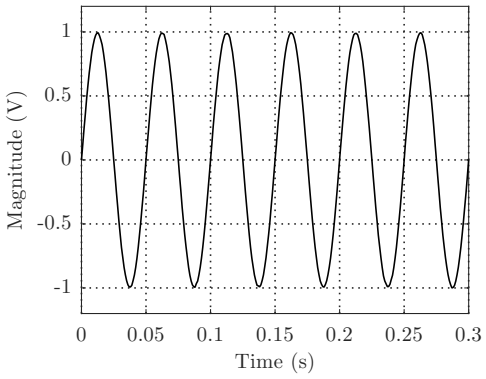

Fig. 39. Signal observed at beamformer output upon using the PSO beamformer.

The PSO beamformer resultant array response pattern is as per Fig. 40.

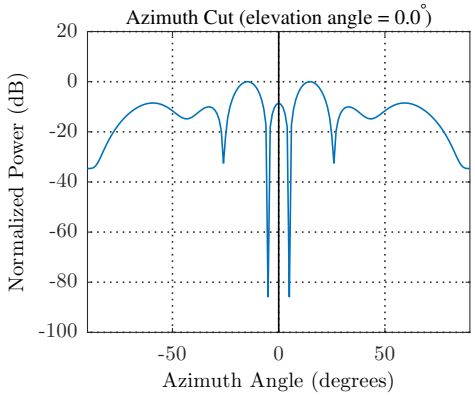

Fig. 40. Beamformer array response upon using the PSO beamformer.

Fig. 41 presents a comparative array response plot.

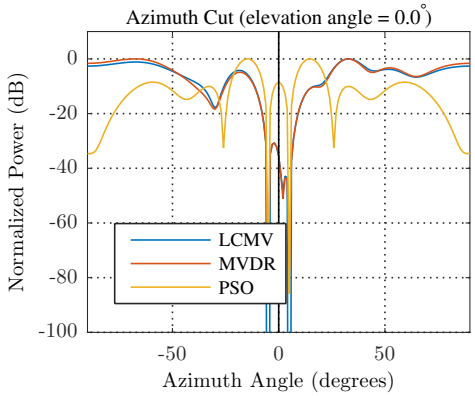

Fig. 41. Comparative array response plot.

From Fig. 41, it is easy to note the superior performance of the PSO solved null-steering beamformer over the MVDR and LCMV beamformers.

E. Overall SINR comparison

Going by Table II, the superior performance of the PSO solved null steering beamformer is evident. The beamformer yields good results even with narrow interferer angular separation. The LCMV beamformer outperforms the MVDR beamformer in all trials.

TABLE II
SINR RESULTS IN DB.

	Trial 1	Trial 2	Trial 3	Trial 4
LCMV Mean	17.643	17.213	16.932	16.789
LCMV Min	9.838	9.330	8.388	8.317
MVDR Mean	14.838	14.522	14.633	14.508
MVDR Min	6.299	5.874	6.872	7.188
PSO Mean	55.284	56.103	56.045	40.420
PSO Min	47.907	48.922	48.500	32.656

VII. CONCLUSION

In this paper, MVDR and LCMV techniques performance comparison has been addressed from the perspective of narrowband beamforming (in reception mode), with the variation parameter being signal/ interferer spatial separation. The LCMV beamformer has been constrained to yield nulls in interferer DoAs. Also studied is a PSO solved null-steering beamformer. From MATLAB software simulations, it has been established that the PSO solved null-steering beamformer outperforms the LCMV and MVDR techniques.

REFERENCES

[1] F. B. Gross, *Smart Antennas for Wireless Communications*. New York: McGraw-Hill, 2nd ed., 2015.
[2] B. Cauchi, I. Kodrasi, R. Rehr, S. Gerlach, A. Jukić, T. Gerkmann, S. Doclo, and S. Goetze, "Combination of mvdr beamforming and single-channel spectral processing for enhancing noisy and reverberant speech," *EURASIP Journal on Advances in Signal Processing*, vol. 2015, p. 61, Jul 2015.
[3] R. Qian, M. Sellathurai, and D. Wilcox, "A study on mvdr beamforming applied to an espar antenna," *IEEE Signal Processing Letters*, vol. 22, pp. 67–70, Jan 2015.
[4] S. Araki, M. Okada, T. Higuchi, A. Ogawa, and T. Nakatani, "Spatial correlation model based observation vector clustering and mvdr beamforming for meeting recognition," in *2016 IEEE International Conference on Acoustics, Speech and Signal Processing (ICASSP)*, pp. 385–389, March 2016.
[5] M. O'Connor, W. B. Kleijn, and T. Abhayapala, "Distributed sparse mvdr beamforming using the bi-alternating direction method of multipliers," in *2016 IEEE International Conference on Acoustics, Speech and Signal Processing (ICASSP)*, pp. 106–110, March 2016.
[6] C. Doroody, S. K. Tiong, and S. Darzi, "Sinr improvement using firefly algorithm (fa) for linear constrained minimum variance (lcmv) beamforming technique," in *2015 International Conference on Computer, Communications, and Control Technology (I4CT)*, pp. 441–445, April 2015.
[7] T. Sherson, W. B. Kleijn, and R. Heusdens, "A distributed algorithm for robust lcmv beamforming," in *2016 IEEE International Conference on Acoustics, Speech and Signal Processing (ICASSP)*, pp. 101–105, March 2016.
[8] A. Hassani, A. Bertrand, and M. Moonen, "Lcmv beamforming with subspace projection for multi-speaker speech enhancement," in *2016 IEEE International Conference on Acoustics, Speech and Signal Processing (ICASSP)*, pp. 91–95, March 2016.
[9] A. Hassani, J. Plata-Chaves, M. H. Bahari, M. Moonen, and A. Bertrand, "Multi-task wireless sensor network for joint distributed node-specific signal enhancement, lcmv beamforming and doa estimation," *IEEE Journal of Selected Topics in Signal Processing*, vol. 11, pp. 518–533, April 2017.
[10] S. Saeed, I. M. Qureshi, A. Basit, A. Salman, and W. Khan, "Cognitive null steering in frequency diverse array radars," *International Journal of Microwave and Wireless Technologies*, vol. 9, no. 1, p. 2533, 2017.
[11] S. N. Monteiro and H.G.Virani, "Improved null steering with sidelobe canceller for linear antenna arrays," *International Journal of Advanced Research in Computer and Communication Engineering*, vol. 4, pp. 97–100, March 2015.